

# **Title:**

The Goldilocks Window of Personalized Chemotherapy:  
 Getting the Immune Response Just Right

## **Authors and Affiliations:**

Derek S. Park<sup>1,2</sup>, Mark Robertson-Tessi<sup>2</sup>, Kimberly A. Luddy<sup>3,4</sup>, Philip K. Maini<sup>5</sup>, Michael  
 B. Bonsall<sup>1</sup>, Robert A. Gatenby<sup>2,6</sup>, Alexander R. A. Anderson<sup>2</sup>

1 – Department of Zoology, University of Oxford, Oxford, United Kingdom

2 – Department of Integrated Mathematical Oncology, H. Lee Moffitt Cancer Center, Tampa, Florida,  
 United States of America

3 - Comparative Immunology Group, School of Biochemistry and Immunology, Trinity College Dublin,  
 Dublin, Ireland

4 - Department of Cancer Physiology, H. Lee Moffitt Cancer Center, Tampa, Florida

5 – Mathematical Institute, University of Oxford, Oxford, Oxfordshire, United Kingdom

6 - Department of Radiology, H. Lee Moffitt Cancer Center, Tampa, Florida, United States of America

## **Corresponding Authors:**

Derek Park  
 12902 USF Magnolia Drive  
 Mailstop: SRB 4  
 Tampa, FL 33612  
 Derek.park@aya.yale.edu  
 813 745-6119

Alexander R. A. Anderson  
 12902 USF Magnolia Drive  
 Mailstop: SRB 4  
 Tampa, FL 33612  
 Alexander.anderson@moffitt.org  
 813 745-6119

**Running title:** The Goldilocks Window of Personalized Chemotherapy

## **Keywords:**

Personalized medicine, tumor-immune interactions, chemotherapy, scheduling, T-cells,  
 homeostatic repopulation

## **Conflict of Interest statement:**

The authors declare no potential conflicts of interest.

## Abstract

The immune system is a robust and often untapped accomplice of many standard cancer therapies. A majority of tumors exist in a state of immune tolerance where the patient's immune system has become insensitive to the cancer cells. Due to its lymphodepleting effects, chemotherapy has the potential to break this tolerance. In order to investigate this, we created a mathematical modeling framework of tumor-immune dynamics. Our results suggest that optimal chemotherapy scheduling must balance two opposing objectives: maximizing tumor reduction while preserving patient immune function. Successful treatment requires therapy to operate in a 'Goldilocks Window' where patient immune health is not overly compromised. By keeping therapy 'just right', we show that the synergistic effects of immune activation and chemotherapy can maximize tumor reduction and control.

## Statement of Significance

To maximize the synergy between chemotherapy and anti-tumor immune response, lymphodepleting therapy must be balanced in a 'Goldilocks Window' of optimal dosing.

## 63 Introduction

64 Immune tolerance occurs when the immune system fails to respond to a target  
 65 despite its potential to induce an immune response. In cancer, this failure leads to  
 66 immune evasion and tumor growth. CD8<sup>+</sup> effector T cells, also known as cytotoxic T  
 67 lymphocytes (CTLs), are an essential component of the adaptive immune system capable  
 68 of responding to tumor antigens and inducing cell death. Immunologically inert tumors  
 69 induce T-cell tolerance through multiple direct mechanisms such as inhibition of  
 70 programmed death ligand 1 (PD-L1), activation of the T-cell regulatory protein CTLA4, and  
 71 production of regulatory cytokines and metabolites [1], as well as indirect methods such  
 72 as recruitment of regulatory T cells (Tregs), myeloid-derived suppressor cells (MDSC) and  
 73 tolerogenic dendritic cells (DC) [2]. Tregs inhibit CTL cytotoxic activity via cell-cell contact  
 74 [3, 4], and through secreted factors such as transforming growth factor beta (TGF-beta) [5,  
 75 6]. They have posed challenges for cancer immunotherapies as well as preventing the  
 76 activation of the immune system during more traditional therapy approaches [4, 7].

77 Breaking tolerance requires removal of multiple suppressive factors and activation  
 78 of cytotoxic immune cells. Chemotherapy, while toxic to CTLs, also has paradoxical and  
 79 important immunostimulatory effects through dysregulation of the immunosuppressive  
 80 tumor microenvironment by reducing regulatory cytokine levels, changes in oxygen levels,  
 81 and reduced metabolites. Several chemotherapies, including cyclophosphamide,  
 82 paclitaxel, gemcitabine, and 5-fluorouracil, can selectively target MDSC and Tregs [8, 9].

83 Additionally, highly cytotoxic chemotherapies with lymphodepleting effects create  
 84 immunologic space [10, 11]. During homeostasis, the body maintains T-cell pools at  
 85 consistent levels. When these pools are depleted, T cells refill this space through antigen-  
 86 independent proliferation, termed homeostatic repopulation, which favors memory T

87 cells [12]. This homeostatic proliferation breaks tolerance, temporarily restoring immune  
 88 response to previously tolerated antigens [13]. This was first characterized in the post-  
 89 transplant setting where memory T cells lose peripheral tolerance during homeostatic  
 90 repopulation, leading to graft rejection [12].

91 Chemotherapy-induced tolerance breaking is dynamic and transient, often  
 92 requiring treatment breaks to achieve full effect. Various studies report that regulatory  
 93 cells return 5-10 days posttreatment [8]. Homeostatic repopulation following moderate  
 94 lymphopenia can fully restore the lymphocyte pool as early as 4 days following therapy in  
 95 murine models [14]. Even in the case of nearly complete lymphodepletion using  
 96 Alemtuzumab in non-human primate transplant models, the T-cell pool is completely  
 97 restored in 8 weeks, consisting of 96% memory T cells [15]. An obvious question then  
 98 arises: is there an optimal chemotherapy schedule that could maximize tumor kill and also  
 99 enhance immune response?

100 To investigate this question, we created a mathematical model of the complex  
 101 tumor-immune dynamics that occur during multiple cycles of chemotherapy. In particular,  
 102 we investigated three, clinically relevant, therapeutic dynamics: immunodepletion,  
 103 immunostimulation via vaccination, and immunosupportive prophylactics. We identified  
 104 significant immune trade-offs during chemotherapy as well as the relevant patient metrics  
 105 that determine the magnitude and severity of these compromises. Further, by exploring  
 106 the impact of clinically-established therapy, as well as more experimental treatment  
 107 decisions, we illustrate a more complex interplay between chemotherapy and patient  
 108 immune dynamics than has been previously investigated. Our results indicate that optimal  
 109 chemotherapy requires identification of a “Goldilocks Window” in which treatment can  
 110 both induce cytotoxic effects in the tumor and enhance the immune response to tumor

111 antigens. Therefore, instead of the one-size-fits-all paradigm of fixed therapy regimens,  
 112 patient immune biology should be a key consideration when developing personalized  
 113 chemotherapy strategies.

## 114 **Materials and Methods**

### 115 **Overall Model Design**

116 A central assumption of this work is that a clinically-detectable tumor has induced  
 117 a tolerant state in which the immune system can no longer respond to tumor antigens.  
 118 Chemotherapy temporarily removes this tolerance through lymphodepletion, which  
 119 eliminates Tregs and allows a burst of immune response. However, the lymphodepletion  
 120 itself also kills CTLs and therefore reduces the potential cytotoxic efficacy. This double-  
 121 edged response to chemotherapy implies that there is an optimal therapeutic strategy.

122 We develop a mathematical model that includes five major populations of cells:  
 123 Tumor cells (***T***), CTLs (***E***), Tregs (***R***), memory T cells (***M***), and naïve T cells (***N***). Immune  
 124 function is separated into two distinct temporal stages, relative to the time of application  
 125 of each chemotherapy cycle: 1) a period of CTL expansion immediately following the  
 126 application of chemotherapy (Figure 1, panel A); and 2) CTL contraction as tolerance  
 127 returns (Figure 1, panel B). The transition time between these phases remains poorly  
 128 characterized, but empirically occurs 5-10 days after the expansion starts [16]. This range  
 129 has been observed in murine models and is dramatic, involving over a 90% decrease in  
 130 population size [17]. A central assumption of this work is that a clinically-detectable  
 131 tumor has induced a tolerant state in which the immune system can no longer respond to  
 132 tumor antigens. Systemic lymphodepletion, including that caused by chemotherapy, can  
 133 help break this tolerance. This can have drastically different effects depending on the type  
 134 and strength of lymphodepletion [18, 19]. First, chemotherapy can selectively reduce

135 Tregs [20, 21, 22] helping to break peripheral tolerance. Second, strong lymphodepletion  
 136 will cause homeostatic proliferation in the lymphoid compartment, further reducing  
 137 tolerance.

138 However, dead immune cells cannot elicit cytotoxic effects or engage in  
 139 homeostatic proliferation. This implies that there is an optimal therapeutic strategy. If the  
 140 dose is too high, then the few remaining immune cells will not be able to take advantage  
 141 of the tolerance breaking; if the dose is too low, then the lymphodepleting effects will be  
 142 insufficient to break tolerance. In addition to these immune effects, the chemotherapy  
 143 itself can induce cancer cell death affecting both the tumor size directly and releasing  
 144 tumor antigens, adding another layer of complexity to the tumor-immune dynamics.

145 Whilst the full course of lymphocyte recoveries are not observed in the treatment  
 146 course, measurements of lymphocyte populations over time have shown that a stable  
 147 equilibrium is reached between chemotherapeutic depletion and population sizes [23].  
 148 Therefore, in the model, there is a window of 5 days immediately following each  
 149 chemotherapy cycle in which the immune system is sensitive, and outside of these  
 150 periods, it is tolerant. We explore the length of this window more thoroughly below.

151 Our efforts to use mathematical modeling to inform chemotherapy build upon  
 152 previous immune and personalized medicine works. Mathematical models of tumor-  
 153 immune activity are numerous, given the complexity of the mechanisms involved (see [24,  
 154 25, 26, 27, 28] for examples relevant to the present work). Explained more fully below, we  
 155 extend the modeling work of Robertson-Tessi et al. [29] to a more clinically-oriented  
 156 setting by simplifying the immunosuppressive dynamics while maintaining Treg  
 157 recruitment and function. There have been efforts to study explicit spatial dynamics of the  
 158 growing cancer cell population in the context of healthy tissue [30, 31]. Here, we

159 implement an implicit spatial limitation on growth (see explanation of  $f(T)$  below); our  
 160 model may be extended in the future to incorporate explicit spatial dynamics. Our initial  
 161 framework choices have been to incorporate patient immune parameters to build towards  
 162 a model for personalized oncology [32].

163 During the phase in which the immune system is sensitive to the tumor, a few key  
 164 processes occur. CTLs, which target and kill the tumor, are recruited from a memory cell  
 165 population due to response to tumor antigens [16]. Recent studies indicate that memory  
 166 T cells make up the majority of T cells engaged in homeostatic repopulation [15, 33].  
 167 These memory cells are constantly undergoing a low level of replenishing proliferation,  
 168 but they only convert to CTLs during the sensitive expansion phase following  
 169 lymphodepletion. During this phase, there is also tumor-mediated recruitment of Tregs.  
 170 This eventually causes a significant shift in immune dynamics, leading to a contraction of  
 171 the CTL compartment during the tolerized phase. Under tolerance, there is no longer a  
 172 significant recruitment of CTLs from the memory cell compartment. Instead, while the  
 173 existing CTLs do carry out some tumor-killing function, the Tregs decrease the CTL  
 174 number.

175  
 176 **Quick guide to equations and assumptions:**  
 177

$$\begin{aligned}\frac{dT}{dt} &= \frac{T}{f(T)} - k_0 \frac{TE}{T+E} \left(1 - b \frac{R}{R+E}\right) \\ f(T) &= \left( \left( \frac{1}{T_{trans}^{m-1} r_T} \right)^P + \left( \frac{T^{1-m}}{r_T} \right)^P \right)^{\frac{1}{P}} \\ \frac{dE}{dt} &= H(t_{off} - t) \left(1 - \frac{M+N}{K_{max}}\right) \gamma \alpha \frac{TM}{T+M} - H(t - t_{off}) \left( \rho E \left(1 + c \frac{R}{R+E}\right) + \delta_E E \right) \\ \frac{dM}{dt} &= r_M M \left(1 - \frac{M+N}{K_{max}}\right) - H(t_{off} - t) \left(1 - \frac{M+N}{K_{max}}\right) \alpha \frac{TM}{T+M} + H(t - t_{off}) \rho \omega E \\ \frac{dR}{dt} &= \sigma T - \delta_R R \\ \frac{dN}{dt} &= r_N N \left(1 - \frac{M+N}{K_{max}}\right)\end{aligned}$$

178

179 Our immune tolerance model assumes that the growth of tumor cells (**T**) can be checked  
 180 by CTLs (**E**). However, CTLs are themselves inhibited by Tregs (**R**) that are recruited at a  
 181 rate  $\sigma$  by tumor antigens. This leads to CTL-mediated tumor cell death being moderated  
 182 by the quantity of Tregs  $\left(\frac{R}{R+E}\right)$ . CTLs exhibit different behaviors during immune expansion  
 183 and immune contraction. This switching behavior is modeled with the Heaviside function  
 184  $\left(H(t_{off} - t)\right)$ . During the immune expansion phase, CTLs are recruited from the memory  
 185 pool based on both available memory cells (**M**) and the tumor burden  $\left(\frac{TM}{T+M}\right)$ . During  
 186 immune expansion, the antigenicity of the tumor ( $\alpha$ ) induces differentiation to CTLs  
 187  $\left(\frac{TM}{T+M}\right)$ . However, as immune tolerance sets in, there is a contraction in the CTL population,  
 188 caused by degradation of CTLs by Tregs (**b**). During immune contraction, CTLs can convert  
 189 back to memory T cells ( $\omega E$ ,  $\omega < 1$ ). Finally, the total remaining lymphocyte population  
 190 that is not sensitive to the tumor (**N**) replicates in a logistic growth model  $r_N N \left(1 - \frac{M+N}{K_{max}}\right)$ .

# 191 Tumor dynamics

$$\frac{dT}{dt} = \underbrace{\frac{T}{f(T)}}_1 - k_0 \underbrace{\frac{TE}{T+E} \left(1 - b \frac{R}{R+E}\right)}_2 \quad (1)$$

192



193 Tumor growth dynamics (term 1) are approximated via a combination of exponential  
 194 growth for smaller tumors and power law growth for larger tumors. This growth model  
 195 includes a few key assumptions about the limitations which a growing tumor faces before  
 196 clinical detection. In the absence of effector cells attacking the tumor population, tumor  
 197 cells first grow exponentially but then transition to power-law growth. This growth  
 198 dynamic is typical of early-stage, preclinical malignant growths and is based on  
 199 mathematical modeling as well as experimental observation [29]. Furthermore, there are  
 200 also practical limitations to the biological validity of the tumor population sizes which the  
 201 model can approximate. While the model can simulate unbounded tumor growth, this is  
 202 obviously clinically impossible due to the resulting morbidity and eventual patient  
 203 mortality. Here, we restrict the analysis to the range of tumor sizes which are typical for  
 204 clinically detectable masses, namely  $T < 10^{10}$  cells. The transition between exponential  
 205 and power law growth dynamics is governed by  $f(T)$  as defined in eq. (2).

$$f(T) = \left( \left( \frac{1}{T_{trans}^{m-1} r_T} \right)^P + \left( \frac{T^{1-m}}{r_T} \right)^P \right)^{\frac{1}{P}} \quad (2)$$

206  
 207 The function  $f(T)$  employs the method of modeling tumor growth in [29]. Beyond a certain  
 208 size ( $T_{trans}$ ), small tumors are not able to sustain their early exponential growth due to  
 209 physical and nutrient limitations, and therefore transition to power law growth at larger  
 210 tumor sizes. The smoothness of this transition is governed by the exponent  $P$ . The  
 211 parameter  $r_T$  represents the tumor growth coefficient.

212 Term 2 of Equation 1 represents the tumor loss due to killing by CTLs. Parameter  $k_0$   
 213 represents the CTL cytotoxic efficacy, with the actual tumor kill rate dependent upon the  
 214 relative numbers of tumor and CTLs  $\left( \frac{TE}{T+E} \right)$ . An estimate of this efficacy was initially set at

1 day<sup>-1</sup> based on the potency of CTLs in preventing tumor growth when stimulated by multiple types of tumor antigen [34]. *In vivo* killing capacities of CTLs have also been measured in the 1 – 10 day<sup>-1</sup> range by real-time imaging in viral systems, although there is significant heterogeneity [35]. However, this rate is mitigated by the presence of Tregs, with ***b*** representing their inhibition efficacy. As Tregs increase in density, the CTL-mediated tumor death rate decreases.

# **CTL dynamics**

$$\frac{dE}{dt} = \underbrace{H(t_{off} - t)}_1 \underbrace{\left(1 - \frac{M + N}{K_{max}}\right)}_2 \underbrace{\gamma \alpha \frac{TM}{T + M}}_3 - \underbrace{H(t - t_{off})}_4 \left( \underbrace{\rho E \left(1 + c \frac{R}{R + E}\right)}_5 + \underbrace{\delta_E E}_6 \right) \quad (3)$$

CTL dynamics are modeled in two phases, expansion (terms 1-3) and contraction into tolerance (terms 4-6). Terms 1 and 4 switch between these phases via the Heaviside function, with ***t<sub>off</sub>*** being the length of the expansion phase (5 days, unless noted) immediately following each round of chemotherapy. Terms 2 and 3 govern the growth of CTLs during immune sensitivity to the tumor. CTLs are generated based upon the antigenicity of the tumor (***α***) as well as the number of tumor and memory cells. Modulating this is an amplification rate, ***γ***, since one memory cell can yield multiple CTLs. Term 2 accounts for the maximum number of lymphocytes that can be supported by the cytokine pool. This paradigm of CTL function being limited by cytokine availability is supported by lymphodepletion studies showing increased CTL activity when IL-7 and IL-15 cytokine-responsive cells were removed [36]. When the immune compartment is full and in homeostasis, this term will be near zero, effectively shutting down CTL recruitment; however, immediately after a dose of chemotherapy, memory and naïve T cells are depleted, which promotes CTL expansion.

Term 5 represents the contraction of the CTL compartment that occurs due to immune tolerance. The death rate of CTLs during contraction,  $\rho$ , is due to decreases in the level of supportive cytokines. This rate is increased by the relative fraction of Tregs that are present,  $\frac{R}{R+E}$ . The modifying constant  $c$  represents the sensitivity of CTL suppression to Tregs through a variety of mechanisms [37]. Lastly, term 6 represents the rate of conversion of CTLs back into memory cells, an active mechanism during immune contraction [38, 39].

### 247 **Memory T cell dynamics**

$$\frac{dM}{dt} = \underbrace{r_M M \left(1 - \frac{M+N}{K_{max}}\right)}_1 - \underbrace{H(t_{off} - t)}_2 \underbrace{\left(1 - \frac{M+N}{K_{max}}\right)}_3 \underbrace{\alpha \frac{TM}{T+M}}_4 + \underbrace{H(t - t_{off})}_{5} \underbrace{\delta_E \omega E}_{6} \quad (4)$$

Memory cells continually replenish themselves through homeostatic growth in term 1. Parameter  $r_M$  is the maximum memory-cell growth rate, subject to a carrying capacity,  $K_{max}$ . During the immune expansion phase (terms 2-4), memory cells convert to CTLs, governed by the relative abundances of tumor and memory cells,  $\frac{TM}{T+M}$ , as well as the antigenicity ( $\alpha$ ). As described in Eq. (3), the rate of recruitment is moderated by the homeostatic fraction of the overall immune system (term 3). During the contraction phase (terms 5 and 6), memory cells are replenished from the CTL compartment. A fraction ( $\omega$ ) of the CTLs is successfully converted back to memory cells [38]. Due to some loss and inefficiency in conversion,  $\omega < 1$  [40].

### 260 **Treg and naïve T cell dynamics**

$$\frac{dR}{dt} = \sigma T - \delta_R R \quad (5)$$

262 Tregs are recruited by tumor cells with rate  $\sigma$ , and they decay with a rate  $\delta_R$  [41, 42].

$$263 \quad \frac{dN}{dt} = r_N N \left( 1 - \frac{M + N}{K_{max}} \right) \quad (6)$$

264 Naïve T-cell dynamics follow homeostatic proliferation with rate  $r_N$ , up to a common  
 265 carrying capacity of  $K_{max}$ , which is the maximum number of memory and naïve T cells in  
 266 the immune system [43].

267 The model was parameterized based on literature sources when possible, as  
 268 shown in Table 1. For many cases, there was evidence of variation in parameters, and  
 269 some cannot be easily measured. Where possible, we have tried to make a biologically  
 270 reasonable order-of-magnitude approximation. In order to address this parameter  
 271 uncertainty we explicitly consider the impact of parameter variation on model results.

272

### 273 **Simulating chemotherapy and evaluating outcomes**

274 To establish tolerance in the system and allow transients from initial conditions to  
 275 dampen before applying therapy, the simulation was initialized with a tumor size of  
 276  $10^7$  cells. Chemotherapy was started when the tumor reached  $10^8$  cells and was simulated  
 277 as periodic doses of cytotoxic therapy at 14-day intervals. In total, 10 cycles of  
 278 chemotherapy were applied. At the time of each treatment cycle, all cell populations  
 279 (immune and tumor) were instantaneously reduced by a fraction  $C_0$  representing the  
 280 cytotoxic effect of chemotherapy on that population. This instantaneous death  
 281 fraction can be understood as lethal dose (LD) values with, for example,  $C_0 = 0.5$   
 282 representing LD<sub>50</sub>. The choice for an instantaneous decrease is simplifying, allowing us to  
 283 omit pharmacodynamics; however this approach reflects the general potency of many  
 284 therapy agents. For example, *in vitro* studies have shown that cellular uptake and

incorporation into RNA for 5-fluorouracil occurs as soon as 3 hours after exposure [44].  
 Uptake levels were directly shown to correlate with cytotoxicity. For doxorubicin,  
 cytotoxicity studies have found that just 1 hour of exposure is enough to induce a 90%  
 decrease in viable, colony forming cells [45].

Immune cells were reduced by the same fraction ( $C_0$ ) on each chemotherapy cycle.  
 However, to account for tumor resistance to therapy, the fractional tumor reduction for  
 cycle  $i$  ( $C_i$ ) was linearly reduced with each cycle, such that the cytotoxic fraction on the last  
 cycle was 75% of the initial fraction  $C_0$ . Approximating the impact of chemoresistance on  
 drug efficacy is challenging since values vary for different classes of drugs. Furthermore,  
 Hao et al. [46] noted dose-dependent differences of up to 400% between resistant and  
 resensitized prostate cancer cell populations to docetaxel. Here, the value of 75%  
 chemotherapy efficacy at the last cycle represents a 33% advantage of survivorship for a  
 resistant population versus a susceptible population. It is a conservative estimate of the  
 impact of resistance, but we believe it is reasonable given that tumor populations are  
 unlikely to be entirely resistant. Varying this range is a relevant question for future  
 research. For our purposes,  $C_i$  is given by:

$$C_i = C_0 \left( 1 - 0.25 \frac{i}{10} \right) \quad (7)$$

The final tumor size after 10 cycles of chemotherapy was compared to the tumor  
 size at the start of treatment ( $10^8$  cells) and evaluated according to RECIST categories.  
 Specifically, a total loss of tumor (<-99% change in size) is a complete response (CR). A  
 change between -30% and -99% is considered a partial response (PR). Tumor changes  
 between -30% and +20% are classified as stable disease (SD) and increases of greater than  
 +20% are seen as progressive disease (PD) [47]. While there are many different methods

of measuring therapy efficacy impact on disease, RECIST categories were chosen here since they have correlated well with overall survival in patients across a variety of cancers.

310

### 311 **Simulation environment**

The model was programmed in the Python language (ver. 2.7.11). The open-source packages Scipy (ver. 0.17.0), Numpy (ver. 1.10.4), and Matplotlib (ver. 1.5.1) were used for simulation of the ODEs as well as visualization of the results. The platform for the program was both an Intel(R) Core (TM) i7-6820 HQ processor as well as the high performance computing cluster at Moffitt Cancer Center, Tampa, Florida, USA. The source code is available at the github repository for the Integrated Mathematical Oncology department at [github.com/MathOnco/Goldilocks](https://github.com/MathOnco/Goldilocks).

319

## 320 **Results**

321

### 322 **Patient memory cell populations determine a ‘Goldilocks Window’ of optimal dosing**

Memory cell population sizes are variable among patients; Arstila et al. have estimated there to be  $10^6 - 10^7$  T-cell clones in the human body with approximately  $10^5$  memory T cells per antigen [29, 48]. However, due to antigen responses being polyclonal, this suggests multiple orders of magnitude of potential variation in memory T-cell numbers. Therefore, varying doses of chemotherapy were simulated for a range of memory cell population sizes (Figure 2A and 2B). Results from the model show that patient memory-cell numbers significantly influence the optimum chemotherapy dose. Generally, there is a minimum memory-cell population size that is necessary for any given strength of chemotherapy to be successful. Above this threshold, the more memory cells there are,

the better the improvement with stronger doses of therapy. Conversely, this means that when memory-cell populations are close to the minimum threshold, chemotherapy should be similarly weak for a more favorable outcome. Furthermore, if memory cells are below the minimum threshold, then the optimal strategy is to use strong chemotherapy (Figure 2A and B), since the immune system will not contribute to tumor regression.

The double-edged nature of chemotherapy on the immune system can be better understood through the transient dynamics during therapy (Figure 2C and D). In cases with stronger chemotherapy dosing, there is an early decrease in tumor population levels due to the cytotoxic strength of the therapy. However, we observe a trend that these strong therapies tend to lead to failure and larger final tumor sizes than if treated with a 'weaker' chemotherapy regimen, which provides lower cytotoxicity on the tumor but maintain tumor size reduction for the duration of therapy.

This counterintuitive result stems from the fact that cytotoxicity alone is insufficient for suppressing tumor growth, especially due to the accumulating chemoresistance. Rather, it is the synergistic effect of cytotoxicity as well as the breaking of immune tolerance and consequent recruitment of CTLs that keeps tumor populations in check. Our *in silico* treatments consistently show that there is an inherent disadvantage to high-dose chemotherapy. There is a gradual decrease in the CTL population over multiple rounds of treatment due to the net loss that stronger dosing causes in memory T-cell populations (Figure 2D). It is these memory cells that are affected the most by chemotherapy since they can only recover relatively slowly. If the cytotoxic pressure on memory cells is greater than the recovery rate of that compartment, then even with a resensitized immune system, expansion will lead to fewer total CTLs and ultimate treatment failure. In contrast, if the immunodepleting side effects of chemotherapy can

356 be balanced with immune recovery, then more sustainable treatment responses are  
 357 possible. In short, there is a tradeoff between having chemotherapy strong enough to  
 358 sufficiently break tolerance, but mild enough to leave sufficient memory T cells for  
 359 adequate CTL expansion. Akin to the story of Goldilocks and the three bears, the balancing  
 360 of these two immunological goals leads to an intermediary chemotherapy strength that is  
 361 'just right'. *In silico* simulation shows that this "Goldilocks Window" is highly dependent  
 362 upon patient-specific, pre-existing memory T-cell populations.

363

364

365 **Patient-specific tumor growth rate and immune strength determine chemotherapeutic**

366 **flexibility**

367 While we identified this Goldilocks Window of optimal, sub-maximal  
 368 chemotherapy dosing, we also sought to explore it in the broader context of patient-  
 369 specific disease and immune variation. For tumor growth rates, we found that successful  
 370 treatment outcomes are more sensitive to chemotherapy dosing for faster growing  
 371 tumors and less sensitive for slower growing tumors. Experimental and model analyses  
 372 have shown that selection pressures on growing tumors can lead to significant  
 373 heterogeneity in metabolism and growth rates [49]. In our framework, the tumor growth  
 374 rate parameter ( $r_T$ ) was set to the maximum speed for doubling during the exponential  
 375 growth phase (1000 cell<sup>-1</sup> per day, representing a doubling time of 1 day), but we also  
 376 explored faster and slower growth rates (Figure 3A and 3B).

377 In slower growing tumors ( $r_T < 1000$ ), chemotherapy's cytotoxic effects are  
 378 sufficient for tumor control. After the partial tumor clearance due to each cycle, there is  
 379 regrowth of the cancer cell population (Figure 2A and B). For slower growing tumors,  
 380 there is less intercycle regrowth and therefore cancer cell populations can be controlled



381 by chemotherapy alone without the need for CTL killing. The result is that, for slower  
 382 growing tumors, there is no Goldilocks Window.

383 However, for faster growing tumors ( $r_T > 1000$ ) it becomes necessary to maintain  
 384 chemotherapeutic strength within the Goldilocks Window in order to achieve optimal  
 385 outcomes. For these tumors, regrowth between chemotherapy doses is significant and  
 386 demands the addition of CTL-mediated tumor killing for disease control. Chemotherapy  
 387 that is stronger than the Goldilocks Window hamstrings the patient's immune activation.

388 Importantly, for the most aggressively growing tumors, there is actually a 'worst-  
 389 case scenario' of intermediary chemotherapy strength (Figure 3B). Here, the worst option  
 390 for chemotherapy is not the strongest possible dose but is instead a 'mid-range' strength  
 391 in treatment. At this chemotherapeutic strength, the drug alone is insufficient to cause a  
 392 reduction in tumor size. However, the dose is still strong enough to lead to severe  
 393 memory cell depletion, undermining any immune efforts at constraining tumor growth.

394 Separate from tumor parameters, patient immune characteristics can also impact  
 395 the sensitivity of treatment outcomes to chemotherapy dosing. One important parameter  
 396 we sought to explore was the rate of CTLs in killing tumor cells ( $k_0$ , Figure 3C and 3D).  
 397 Without changing the initial patient memory-cell populations ( $M_0 = 10^6$ ), or the tumor  
 398 growth rate ( $r_T = 1000$ ), the CTL-mediated cytotoxicity rate was varied around the  
 399 biologically realistic parameter of  $k_0 = 0.9$  [34]. CTL efficacy was found to dramatically  
 400 impact sensitivity chemotherapy dosing and the Goldilocks Window. Lower rates of CTL-  
 401 mediated tumor cell death lead to greater sensitivity of treatment outcomes on  
 402 chemotherapy dosing (Figure 2C and D). With a lower value of  $k_0$ , more CTLs are necessary  
 403 to exert the same degree of immune control over the tumor. However, strong  
 404 chemotherapy on a patient with lower  $k_0$  values prevents sufficient CTL expansion by

405 rapidly diminishing the memory-cell populations. Higher CTL killing rates, though,  
 406 removed the restriction of this Goldilocks Window and made successful treatment  
 407 outcomes less sensitive to dosing. While higher chemotherapy doses may lead to larger  
 408 immune depletion, more efficient CTLs mean that these smaller immune populations still  
 409 lead to successful treatment outcomes.

410 In addition, we examined the impact of changing the window duration for immune  
 411 expansion immediately following each chemotherapy dose. Current literature indicates  
 412 that immune contraction can begin to occur anywhere from 4 to 8 days after treatment [8,  
 413 14, 17]. When these extremes were explored (see Figure S1), there was no significant  
 414 qualitative difference to our observation of a sub-maximal optimal dosing range when  
 415 compared between 4 days (Figure S1A) and 8 days (Figure S1B). While a longer window of  
 416 immune expansion (Figure S1B) leads to more favorable outcomes for more rapidly  
 417 growing tumors when treated in the optimal dosing range, the actual presence of this sub-  
 418 maximal dosing range does not change. Furthermore, there is almost no difference in the  
 419 outcomes of patients who are overtreated. This also implicitly addresses our  
 420 mathematical implementation of a switch via a Heaviside Function. Specifically, while  
 421 there might be any number of less abrupt and more gradual transitions between immune  
 422 expansion and immune contraction, our exploration of the dynamics at the extremes of  
 423 this transition range would give an idea of what the intermediate behaviors due to a  
 424 smoother transition might cause. That is, our qualitative results would not significantly  
 425 change with a smoother function.

426 In a broader exploration of the model's immune parameters, a general trend was  
 427 observed that a more robust immune response would improve the outcome (Figures S2-  
 428 S7). For certain model parameters that were more difficult to accurately estimate from

the literature, we explored their variation for the default tumor growth rate and a chemotherapy strength of 25%. If the patient had a stronger immune system characterized by lower CTL death rate ( $\delta_E$ ), lower sensitivity to Tregs ( $c$ ), greater memory cell expansion ( $\gamma$ ), regrowth ( $r_M$ ), and back-conversion ( $\omega$ ), the final tumor population was smaller. Furthermore, more robust anti-tumor immune responses led to greater maximum possible reductions over the range of chemotherapy. In addition, these changes led to expansions of the Goldilocks Window in terms of chemotherapy doses that could achieve tumor reductions.

In short, patient-specific disease and immune biology determines the sensitivity of treatment outcomes to chemotherapy dosing. For rapidly growing tumors, chemotherapy must be maintained in a sub-maximal Goldilocks Window to optimize drug and immune synergies. However patient immune biology matters as well, with weaker immune characteristics also leading to a greater necessity to stay within the Goldilocks Window. Importantly, this presents potentially counterintuitive guidance since an initial motivation may suggest that, in a situation where a patient has a weaker immune system, chemotherapy strength should be increased in order to compensate. However, our model suggests that the lymphodepleting impact of heavy chemotherapy on an already weakened immune system will only worsen outcomes. When confronted with weaker patient immune systems, chemotherapy needs to be maintained within the Goldilocks Window for successful outcomes.

449

#### 450 **Improvements to therapy outcomes from immunostimulatory vaccines**

Patient-specific vaccines have become a recent hallmark in personalized cancer therapy. One of the first to acquire FDA approval was Sipuleucel-T, for treating metastatic

castrate resistant prostate cancer [50]. Each vaccine is tailored to a specific patient by culturing dendritic cells from patients using a specific tumor antigen. Reinjection into the patient would potentially stimulate a T-cell mediated antitumor immune response. Three doses were administered in 2 week intervals with significant clinical responses being observed. Vaccination led to a 22% reduction in the relative risk of death, although there was no noticeable decrease in the rate of progression of disease [50]. The specific effect on T cells was quantified by looking at T-cell receptor changes in response to vaccination. Certain receptor sequences were enriched, while others were significantly decreased [51], suggesting that the vaccine promoted an antigen-specific immune response against the tumor.

To study the effects and potential synergy of chemotherapy with this method of T-cell stimulation, we simulated a vaccine regime similar to that used for Sipuleucel-T (3 doses, spaced 14 days apart), with different vaccine strengths. Mathematically, this was modeled by modifying the ODEs that govern CTL expansion, without explicitly representing the complex DC-to-T-cell cascade that the vaccine induces. Other models have examined the DC cascade in more detail. For example, the explicit migration of dendritic cells between blood, spleen, and tumor have been modeled via delay-differential equations in order to better characterize the specific dose timing-dependent responses to therapy [28]. For simplicity, here we focus solely on the net effect of the vaccine on T-cell numbers by changing the antigenicity parameter of the tumor,  $\alpha$ , from a constant coefficient to a variable, time-dependent function,  $\alpha_v(t)$ :

$$\alpha_v(t) = \alpha + v \left( \frac{1}{2} \right)^{\frac{t}{t_{half}}} \quad (9)$$

475 Total antigenicity is modeled as the result of both the constant, baseline antigenicity of  
 476 the tumor,  $\alpha$ , and an exponentially decaying vaccine-augmented component,  $v$ , which  
 477 decays with a half-life,  $t_{half} = 3$  days, a biologically realistic timespan [52]. This model of  
 478 dynamic antigenicity can be expanded for multiple vaccinations, as used in the clinical  
 479 protocol (Eq. 10).

$$\alpha_v(t) = \alpha + \sum_{n=1}^{n_{vac}} H(t - t_n) v \left( \frac{1}{2} \right)^{\frac{t-t_n}{t_{half}}} \quad (10)$$

480  
 481 Here,  $H(t)$  is again the Heaviside function. The constant  $n_{vac}$  represents the total number  
 482 of vaccine injections and  $t_n$  represents the time of the  $n^{th}$  vaccination. The ODEs used for  
 483 the simulation of immune and tumor cell populations are then dependent on the  
 484 instantaneous current value of  $\alpha_v(t)$  throughout the course of simulated therapy.

485 Here, we explored a range of antigenic increases due to potential patient-to-  
 486 patient variation in responses to immunostimulatory vaccines. While dendritic cell  
 487 vaccines like Sipuleucel-T administer all of the available dendritic cells, responses in  
 488 individual patients vary in how much the antigenicity is changed. In our range of  
 489 exploration, though, we found some commonalities in vaccine interaction for  
 490 chemotherapy.

491 Results show that vaccine therapy can improve outcomes, but only within a  
 492 specific range of chemotherapy strengths (Figure 4). Treatment outcomes improve when a  
 493 vaccine is used with moderate chemotherapy (Figure 4A), but for very high chemotherapy  
 494 doses, the beneficial effects of a vaccine are diminished. As before, the underlying cause  
 495 for decreasing efficacy is the persistent lymphodepletion due to the chemotherapy.  
 496 Antigenicity augmentation due to vaccine stimulation is offset by reduced CTL expansion.  
 497 However, very low-dose chemotherapy poses its own challenges, because with insufficient

lymphodepletion, tolerogenic mechanisms and greater Treg recruitment inhibit any CTL response augmented by the vaccine. The immune system remains closer to tumor-tolerized homeostasis, and as a result vaccine stimulation is mitigated because the immune system is already suppressed. Therefore, the width of the optimal window is not significantly affected by the vaccine, since the vaccine has no effect on a highly depleted or tolerized immune system.

Therefore, even with immunostimulatory vaccines, there exists an optimal “Goldilocks” Window. Quantitatively, we define this window to be the region in which a therapy dose can offer at least a 20% reduction in tumor size since this is the necessary amount for disease to become classified as a partial response. In order for there to be this maximized benefit from vaccine application, the chemotherapy regimen must be ‘just right’. Chemotherapy must have sufficient lymphodepletion to resensitize the immune system, but must leave enough immune cells such that vaccine stimulation leads to a large CTL response. Similar to the results of chemotherapy without the vaccine, the specific range of this Goldilocks Window depends upon the initial patient memory cell ( $M_0$ ) numbers.

We note that the small oscillations observed in the plots (Figure 4B) are a result of the use of dual growth laws for the tumor. Essentially, giving the vaccine causes the tumor to dip into the faster exponential growth phase at an earlier chemo cycle than when chemo is given alone. Since the chemo cycles are discrete and instantaneous, this generates an effective step function to the response with increasing chemo dose, superimposed on the single-peaked optimal curve; this step function is further rounded by both the smoothing exponent  $P$  between the growth laws and the non-linear interactions between tumor growth and immune response at small tumor sizes.

522 **Impact of variation in immune support**

523 Chemotherapeutic lymphodepletion in the clinical setting can pose a serious threat to the  
 524 safety of the patient through neutropenia [53], which commonly leads to dose reductions  
 525 and disruptions to the standard schedule of therapy for patients. Consequently, multiple  
 526 tools have been developed to help mitigate the effects of chemotherapy on the immune  
 527 system. For example, it was recognized that dexamethasone treatment before carboplatin  
 528 and gemcitabine could not only increase chemotherapy efficacy but also reduce the  
 529 lymphodepleting effects by preventing uptake in the spleen and bone marrow [54]. In  
 530 contrast, other aspects of cancer therapy can potentially hamper CTL responses to tumor  
 531 insults. For example, G-CSF application has been shown to reduce CTL activation and could  
 532 conceivably impede the impact of lymphodepletion as a break from immune tolerance  
 533 [55, 56]. More generally, however, the broader impact of immune system augmentation  
 534 or suppression during therapy remains unexamined.

535 In order to examine the effect of attenuated or augmented lymphodepletion on  
 536 therapy outcome, we allowed for variable chemotherapeutic toxicity to immune  
 537 populations, as compared to the tumor population. Mathematically, this simply means  
 538 modifying the chemotherapy dose by a scaling factor  $h$ . The effect of chemotherapy on  
 539 immune cell populations at a given treatment time is:

$$540 \quad I_1 = I_0(1 - hC) \quad (8)$$

541 where  $I_1$  is the immunological population size after application of chemotherapy,  $I_0$  is the  
 542 population size before therapy, and  $0 < C < 1$  is the dose strength. The specific numerical  
 543 range in which  $h$  falls represents either attenuated or augmented chemotherapeutic  
 544 toxicity. For values of  $0 < h < 1$ , this represents an attenuated toxicity on the immune

545 system relative to the toxicity on the tumor. In contrast, values of  $h > 1$  represent higher  
 546 toxicity on patient immune populations than on the tumor. This could be due to patient-  
 547 dependent increased sensitivity to chemotherapy. The maximum possible reduction of  
 548 cells by chemotherapy when modified by immune support is 100%. This leads to the  
 549 resulting condition that  $hC < 1$ . For our *in silico* therapies,  $h$  was varied across the  
 550 allowable ranges for three different strengths of chemotherapy. Values of  $C$  were chosen  
 551 to represent lower ( $C = 0.25$ ), middle ( $C = 0.6$ ), and higher ( $C = 0.9$ ) dose chemotherapy  
 552 (Figure 5A).

553 Interestingly, the results suggest that immune-supporting combination therapy has  
 554 essentially no benefit when given with low dose chemotherapy. As shown in Figure 5,  
 555 similar tumor reduction occurred for a wide range of values of  $h$  around  $h = 1$ .  
 556 Furthermore, outcomes were worse when  $h$  was very low or very high. In situations where  
 557 it was very low, final tumor sizes were large because a lack of lymphodepletion did not  
 558 sufficiently break immune tolerance. In contrast, for larger  $h$  values, there was over-  
 559 depletion which prevented an effective immune response despite significant tolerance  
 560 breaking.

561 In contrast, high dose chemotherapy saw treatment failure or success highly  
 562 dependent upon the amount of immune support. Similar to low dose therapy, a small  
 563 value of  $h$  that mitigated the depleting effects of chemotherapy led to the best possible  
 564 outcomes in terms of tumor shrinkage. Final tumor sizes were, in fact, multiple orders of  
 565 magnitude lower than was possible with low-dose chemotherapy. As  $h$  increased  
 566 (representing less toxicity mitigation) treatment outcomes rapidly worsened. The  
 567 transition value  $h^*$ , where the clinical outcome rapidly shifts, indicates a threshold effect  
 568 with regard to immune support. For high chemotherapy doses, immune support



569 treatments must have a significantly large mitigation ( $h < h^*$ ) of immunodepletion in order  
 570 for successful treatment responses to occur. The position of this inflection point is  
 571 influenced by the strength of the patient immune system to begin with. In expanded  
 572 parameter analyses, the strength or weakness of the simulated patient's immune system  
 573 led to changes in the upper bound of the Goldilocks Window (Figures S2 – S7).

574         The moderate strength chemotherapy regimen yielded only partial benefits of  
 575 either extreme. The greatest tumor reduction possible, with immune support, yielded  
 576 tumors that were smaller than those achievable with low dose chemotherapy. However,  
 577 these tumors were still multiple orders of magnitude larger than those achievable with  
 578 high dose chemotherapy. For treatment failure at lower immune support ( $h > h^*$ ) tumor  
 579 sizes were actually larger than when high dose chemotherapy failed.

580         Clinically, the results suggest that chemotherapy dose strength can be used to  
 581 mitigate uncertainty regarding the amount of immune support a certain treatment will  
 582 give to a specific patient. Low dose therapy offers a wide range of potential immune  
 583 support in which treatment can successfully reduce tumor sizes. The disadvantage is that  
 584 the maximum tumor size reduction still leaves larger tumors than are possible using  
 585 higher doses of chemotherapy. While our model has not analyzed this, a potential impact  
 586 is that larger tumor sizes could lead to more heterogeneous populations and thus lead to  
 587 a higher likelihood of resistant or metastatic populations. However, higher doses have a  
 588 narrower range of immune support in which they are successful. Chemotherapy can be  
 589 balanced, then, against how certain the clinician is of the benefit that G-CSF (or other  
 590 immune supporting drug) will give. For patients where there is high certainty of a  
 591 significant benefit due to the drug, high dose therapy is optimal. In contrast, lower dosing  
 592 should be used when the drug may have lower or variable efficacy.

593 Finally, we sought to investigate how variation in the effectiveness of these  
 594 immune adjuvants might impact treatment outcomes in a group of patients.  
 595 Chemotherapy treatment leads to a wide range of responses, both successful and  
 596 unsuccessful, across multiple types of cancer [47]. This variation has been attributed to  
 597 both disease variation, patient variation, and interactions between the two. However, less  
 598 attention has been given to variable patient responses to secondary drugs – such as G-CSF  
 599 – and how they impact therapy. Patient responses to these secondary drugs are currently  
 600 poorly measured and could have significant implications for therapy outcomes.

601 To better explore the effect of variable patient responses to immune support  
 602 drugs, cohorts of 500 patients were randomly generated from a normal distribution with a  
 603 mean immune support response value of  $h = 0.8$  and variance of 0.2. These values were  
 604 chosen to center the distribution around the model-derived threshold value  $h^* = 0.8$ .  
 605 While not directly describing patient responses to immune support drugs, a normal  
 606 distribution for selection was chosen due to the fact that immune cell counts have been  
 607 found to be normally distributed in population cohorts [57].

608 Similar to our previous investigations, cohorts were then subjected to regimens of  
 609 low ( $C = 0.4$ ) and high ( $C = 0.8$ ) chemotherapy strengths (Figure 5B). Percent changes in  
 610 tumor size after therapy were displayed for each individual patient in the cohort to  
 611 generate a waterfall plot. In doing so, we used our model to simulate cohort responses as  
 612 is commonly measured in aggregated studies of patient data [47]. The waterfall plots  
 613 (Figure 5) illustrate that chemotherapy strength can significantly change the proportion of  
 614 successfully responding patients in a population with variable responses to immune  
 615 prophylactics. This is significant since the proportion of successful responses is often an  
 616 important criterion for judging therapeutic efficacy. The simulated waterfall plots show

617 how clinical outcomes could not only be the result of therapy, but also due to inherent  
 618 immune variation within the cohort.

## 619 Discussion

620

621 A major barrier to success for immunotherapy in cancer is tolerogenic mechanisms  
 622 that reduce the immune response to tumor antigens [58, 4, 7]. A potential solution has  
 623 come from observations that lymphodepletion stimulates homeostatic proliferation in the  
 624 immune system which can transiently restore an immune response. This has led to  
 625 increasing efforts to selectively apply chemotherapy to improve outcomes from  
 626 immunotherapy [59].

627 To better understand this potential synergy, we constructed a mathematical model  
 628 to frame these complex dynamics and identify critical parameters that govern the clinical  
 629 outcomes. Our studies focused on three clinically-observed dynamics of  
 630 immunodepletion, immunostimulatory vaccination, and immunosupportive prophylactics.  
 631 With regard to immunodepletion, we demonstrated that chemotherapy results in a trade-  
 632 off. At very high doses, chemotherapy has a maximal cytotoxic effect on the tumor but  
 633 also maximally depletes T cells such that no effective CTL response can be mounted  
 634 despite the transient loss of tolerance during re-expansion of the immune cells after  
 635 completion of chemotherapy. Similarly, low doses of chemotherapy are insufficient to  
 636 produce the post-treatment immune cell expansion that is necessary for reversal of  
 637 immune tolerance.

638 Importantly, however, we find there is a Goldilocks Window of chemotherapy  
 639 doses in which lymphodepletion causes adequate immune resensitization, but does not  
 640 impose an overly large recovery burden. This window is governed by the patient-specific

641 quantity of memory T cells so that larger pre-treatment T-cell populations allow more  
 642 favorable outcomes with higher doses of chemotherapy. In contrast, fewer pretreatment  
 643 CTLs can limit the immune response even in the Goldilocks window of chemotherapy.  
 644 Thus, there is a necessary 'minimum efficacy' of CTLs for successful stimulation of immune  
 645 response by chemotherapy. Below this threshold of immune activity, the benefit of  
 646 chemotherapy is almost solely dependent on its inherent cytotoxicity (Figure 6).

647 Our model also provides insight into the potential effects of variation in the tumor  
 648 growth rate. In slower growing tumors, chemotherapy alone can be sufficient to achieve  
 649 optimal treatment response. Treatment of faster growing tumors, however, is best when  
 650 the chemotherapy is administered to enhance the immune response. Unfortunately, if the  
 651 pre-treatment population of CTLs is small, we find chemotherapy for rapidly growing  
 652 tumors will be ineffective if it is both highly lymphodepleting and insufficiently cytotoxic to  
 653 significantly reduce tumor growth. Assessing the clinical importance of this question is  
 654 challenging because it remains unclear from the literature as to the actual size of the  
 655 population of tumor-specific T cells that are present during treatment. In spite of these  
 656 difficulties, the impact and existence of anti-tumor immunity has been bolstered by recent  
 657 immunotherapies which act to remove inhibitions to T-cell action [60].

658 Chemotherapy is increasingly being used in concert with vaccines to help stimulate  
 659 the patient immune system. We investigated the interactions between vaccines and  
 660 lymphodepletion and found that, as before, there is a window of chemotherapy ranges in  
 661 which vaccines can improve outcomes versus chemotherapy alone. At very high doses,  
 662 however, the resulting lymphodepletion substantially reduces benefits of immune  
 663 stimulation by vaccination. More broadly, other novel immunotherapies could also  
 664 potentially be hampered by over-depletion of the immune system.

665 To further investigate the potential impact of this interaction, we modeled the  
 666 effect of differential responses to immune prophylactics. G-CSF and other drugs have  
 667 become common recourses in chemotherapy for mitigating the immunodepletion effects  
 668 on patients [61]. However, recent studies have suggested that T cell response is  
 669 hampered by G-CSF administration [55]. While G-CSF may help prevent neutropenia and  
 670 cytopenia for patients, it may impede the ability of retolerized T cells to mount an anti-  
 671 tumor response. In addition, responses to prophylactics are not constant but the  
 672 significance of this variation remains relatively uninvestigated. Our model suggests that  
 673 inter-patient variation in prophylactic response can lead to drastically different outcomes  
 674 for the same dosing of chemotherapy. Across larger samples, this variation can further  
 675 interact with chemotherapy to be a significant determinant of whether the chemotherapy  
 676 dose leads to more success or failure across a range of patients.

677 In the clinical literature, our model results cautioning about balancing  
 678 chemotherapy and immunogenic effects has been echoed in multiple situations. Previous  
 679 studies have explored the mechanisms of action in monoclonal antibody-based  
 680 treatments including targeting of HER2 [62, 63]. When quantifying the impact of  
 681 antibody-dependent cytotoxicity mediated by CTLs, it was noted that addition of paclitaxel  
 682 reduced the lasting impact of the immune response generated against the tumor. While in  
 683 the short term higher doses of chemotherapeutic agents could induce larger tumor  
 684 reductions, mice that were given both antigen and large chemotherapy doses were more  
 685 susceptible to tumor rechallenge. Similarly, in radiotherapy it has been found that CTL  
 686 priming occurs due to antigen-dependent cell death [64]. However, the addition of even a  
 687 small amount of paclitaxel was found to induce a significant reduction in CTL numbers.  
 688 Adjuvant chemotherapy regimens were found to significantly abrogate the immunogenic

689 benefits of radiotherapy-induced immune responses, while immunotherapies increased  
 690 the efficacies. This result is also significant because it implicitly addresses whether our  
 691 results might hold when antigen increase, due to cell death, is accounted for. In this  
 692 mouse model, even with tumor-cell-death-mediated antibodies, the loss of T cells leads to  
 693 a worse overall outcome [64]. This presents a natural extension of our framework to be  
 694 applied to a specific disease and chemotherapy dosing setting. While we created a general  
 695 model of chemotherapy, there may be interesting dynamics unique to individual cancers  
 696 that could be explored. It would also allow the employment of more complex  
 697 pharmacodynamics modeling for specific treatment regimens.

698 In conclusion, our results suggest opportunities to increase the efficacy of  
 699 immunotherapy with precise application of chemotherapy. Our model affirms the  
 700 importance of CTL and memory T-cell expansion following chemotherapy to reduce  
 701 immune tolerance to tumor antigens. However, we demonstrate that optimal  
 702 chemotherapy requires identification of a Goldilocks Window in which treatment can both  
 703 induce cytotoxic effects in the tumor and enhance the immune response to tumor  
 704 antigens. Identifying optimal strategies for chemotherapy in each patient will likely benefit  
 705 from the application of mathematical models which are parameterized by patient data  
 706 pre-treatment to generate an optimal treatment strategy for that patient. Importantly,  
 707 these predicted strategies would most likely need to change as patient responses diverge  
 708 from those predicted, leading to an iterative loop of 'predict-apply-refine'. With the  
 709 growing drive towards precision medicine, we believe that mathematical models are  
 710 critical for the future of truly personalized therapy, where no two patients will receive the  
 711 same therapeutic regimen, and where treatments adapt a change based on patient  
 712 responses. The model presented here is a step towards describing the complex landscape

713 of treatment decisions regarding dosing and combination of different therapies, and we  
714 have shown how these decisions can be sensitive to patient-specific parameters and guide  
715 clinical intuition.

716

## 717 **Acknowledgements**

718

719 D. Park was supported by a 2014 Marshall Scholarship from the Marshall Aid  
720 Commemoration Commission of Great Britain. A. R. Anderson, R. A. Gatenby, M.  
721 Robertson-Tessi, and K. A. Luddy, were supported by a Physical Sciences-Oncology Center  
722 grant from the National Cancer Institute of the United States of America (grant number  
723 1U54CA193489) and the Center of Excellence for Evolutionary Therapy at H. Lee Moffitt  
724 Cancer Center and Research Institute.

## References

- [1] Y. Xing and K. A. Hongquist, "T-cell tolerance: central and peripheral.," *Cold Spring Harb Perspect Biol.*, vol. 4, no. 6, 2012.
- [2] R. Nurieva, J. Wang and A. Sahoo, "T-cell tolerance in cancer," *Immunotherapy*, vol. 5, no. 5, pp. 513-531, 2013.
- [3] A. Corthay, "How do Regulatory T Cells Work?," *Scand J Immunol*, vol. 70, no. 4, pp. 326-336, 2009.
- [4] A. Tanaka and S. Sakaguchi, "Regulatory T cells in cancer immunotherapy," *Cell Research*, vol. 27, pp. 109-118, 2017.
- [5] D. Thomas and J. Massgue, "TGF-beta directly targets cytotoxic T cell functions during tumor evasion of immune surveillance," *Cancer Cell*, vol. 8, no. 5, pp. 369-80, 2005.
- [6] S. McKarns and R. Schwarz, "Distinct effects of TGF-beta 1 on CD4(+) and CD8(+) T cell survival, division, and IL-2 production: A role for T cell intrinsic Smad3," *J Immunol*, vol. 174, no. 4, pp. 2071-83, 2005.
- [7] Y. Takeuchi and H. Nishikawa, "Roles of regulatory T cells in cancer immunity," *Int Immunol*, vol. 28, no. 8, pp. 401-9, 2016.
- [8] Y. Zheng, Y. Dou, L. Duan, C. Cong, A. Gao, Q. Lai and Y. Sun, "Using chemo-drugs or irradiation to break immune tolerance and facilitate immunotherapy in solid cancer," *Cellular Immunology*, vol. 294, pp. 54-59, 2015.
- [9] A. M. Cook, W. J. Lesterhuis, A. K. Nowak and R. A. Lake, "Chemotherapy and immunotherapy: mapping the road ahead," *Current Opinion in Immunology*, vol. 39, pp. 23-29, 2016.
- [10] J. W. Hodge, C. T. Garnett, B. Farsaci, C. Palena, K.-Y. Tsang, S. Ferrone and S. R. Gameiro, "Chemotherapy-induced immunogenic modulation of tumor cells enhances killing by cytotoxic T lymphocytes and is distinct from immunogenic cell death," *International Journal of Cancer*, vol. 133, pp. 624-636, 3 2013.
- [11] L. Bracci, G. Schiavoni, A. Sistigu and F. Belardelli, "Immune-based mechanisms of cytotoxic chemotherapy: implications for the design of novel and rationale-based combined treatments against cancer," *Cell Death and Differentiation*, vol. 21, pp. 15-25, 2014.
- [12] N. K. Tchao and L. A. Turka, "Lymphodepletion and Homeostatic Proliferation: Implications for Transplantation," *American Journal of Transplantation*, vol. 12, pp. 1079-1090, 3 2012.
- [13] C. Wrzensinski, C. Paulos, A. Kaiser, P. Muranski, D. Palmer, L. Gattinoni, Z. Yu, S. Rosenberg and N. Restifo, "Increased intensity lymphodepletion enhances tumor treatment efficacy of adoptively transferred tumor-specific T cells," *J Immunother*, vol. 33, no. 1, pp. 1-7, 2010.
- [14] S. R. Gameiro, J. A. Caballero, J. P. Higgins, D. Apelian and J. W. Hodge, "Exploitation of differential homeostatic proliferation of T-cell subsets following chemotherapy to enhance the efficacy of vaccine-mediated antitumor responses," *Cancer Immunol Immunother.*, vol. 60, no. 9, pp. 1227-1242, 2011.
- [15] M. R. Marco, E. M. Dons, D. J. van der Windt, J. K. Bhamra, L. T. Lu, A. F. Zahorchak, F. G. Lakkis, D. K. Cooper, M. B. Ezzelerab and A. W. Thomson, "Post-transplant repopulation of naïve and memory T cells in blood and lymphoid tissue after alemtuzumab-mediated depletion in heart-transplanted cynomolgus monkeys," *Transpl Immunol.*, vol. 29, no. 1-4, pp. 88-98, 2013.
- [16] C. Althaus, V. Ganusov and R. De Boer, "Dynamics of CD8(+) T cell responses during acute and chronic lymphocytic choriomeningitis," *J Immunol*, vol. 17, no. 9, pp. 2944-51, 2007.
- [17] R. H. Schwarz, "Historical Overview of Immunological Tolerance," *Cold Spring Harb Perspect Biol.*, vol. 4, no. 4, 2012.
- [18] D. Alizadeh and N. Larmonier, "Chemotherapeutic Targeting of Cancer-Induced Immunosuppressive Cells," *Cancer Research*, vol. 74, pp. 2663-2668, 4 2014.



- [19] M. E. C. Lutsiak, "Inhibition of CD425 T regulatory cell function implicated in enhanced immune response by low-dose cyclophosphamide," *Blood*, vol. 105, pp. 2862-2868, 4 2005.
- [20] W. Dummer, A. G. Niethammer, R. Baccala, B. R. Lawson, N. Wagner, R. A. Reisfeld and A. N. Theofilopoulos, "T cell homeostatic proliferation elicits effective antitumor autoimmunity," *Journal of Clinical Investigation*, vol. 110, pp. 185-192, 7 2002.
- [21] A. Schietinger, J. J. Delrow, R. S. Basom, J. N. Blattman and P. D. Greenberg, "Rescued Tolerant CD8 T Cells Are Preprogrammed to Reestablish the Tolerant State," *Science*, vol. 335, pp. 723-727, 1 2012.
- [22] J. Kline, I. E. Brown, Y.-Y. Zha, C. Blank, J. Strickler, H. Wouters, L. Zhang and T. F. Gajewski, "Homeostatic Proliferation Plus Regulatory T-Cell Depletion Promotes Potent Rejection of B16 Melanoma," *Clinical Cancer Research*, vol. 14, pp. 3156-3167, 5 2008.
- [23] H. Meir, R. A. Nout, M. J. P. Welters, N. M. Loof, M. L. Kam, J. J. Ham, S. Samuels, G. G. Kenter, A. F. Cohen, C. J. M. Melief, J. Burggraaf, M. I. E. Poelgeest and S. H. Burg, "Impact of (chemo)radiotherapy on immune cell composition and function in cervical cancer patients," *OncolImmunology*, vol. 6, p. e1267095, 2 2017.
- [24] K. P. Wilkie and P. Hahnfeldt, "Modeling the Dichotomy of the Immune Response to Cancer: Cytotoxic Effects and Tumor-Promoting Inflammation," *Bulletin of Mathematical Biology*, vol. 79, pp. 1426-1448, 6 2017.
- [25] X. Lai and A. Friedman, "Combination therapy of cancer with cancer vaccine and immune checkpoint inhibitors: A mathematical model," *PLOS ONE*, vol. 12, p. e0178479, 5 2017.
- [26] R. Eftimie, J. Dushoff, B. W. Bridle, J. L. Bramson and D. J. D. Earn, "Multi-Stability and Multi-Instability Phenomena in a Mathematical Model of Tumor-Immune-Virus Interactions," *Bulletin of Mathematical Biology*, vol. 73, pp. 2932-2961, 4 2011.
- [27] U. Ledzewicz, M. Naghnaeian and H. Schättler, "Optimal response to chemotherapy for a mathematical model of tumor-immune dynamics," *Journal of Mathematical Biology*, vol. 64, pp. 557-577, 5 2011.
- [28] L. DePillis, A. Gallegos and A. Radunskaya, "A Model of Dendritic Cell Therapy for Melanoma," *Frontiers in Oncology*, vol. 3, 2013.
- [29] M. Robertson-Tessi, A. El-Kareh and A. Goriely, "A mathematical model of tumor-immune interactions.," *Journal of Theoretical Biology*, vol. 294, pp. 56-73, 2012.
- [30] L. G. De Pillis and A. Radunskaya, "The dynamics of an optimally controlled tumor model: A case study," *Mathematical and Computer Modelling*, vol. 37, no. 11, pp. 1221-1244, 2003.
- [31] P. Hinow, P. Gerlee, L. J. McCawley, V. Quaranta, M. Ciobanu, S. Wang, J. M. Graham, B. P. Ayati, J. Claridge, K. R. Swanson, M. Loveless and A. R. A. Anderson, "A spatial model of tumor-host interaction: application of chemotherapy.," *Mathematical biosciences and engineering : MBE*, vol. 6, no. 3, pp. 521-546, 7 2009.
- [32] S. Hamis, G. G. Powathil and M. A. J. Chaplain, "Blackboard to Bedside: A Mathematical Modeling Bottom-Up Approach Toward Personalized Cancer Treatments.," *JCO Clin Cancer Inform.*, no. 3, pp. 1-11, 2019.
- [33] K. P. Cheung, E. Yang and A. W. Goldrath, "Memory-Like CD8 T Cells Generated during Homeostatic Proliferation Defer to Antigen-Experienced Memory Cells," *The Journal of Immunology*, vol. 183, pp. 3364-3372, 8 2009.
- [34] A. Diefenbach, E. Jensen, A. Jamieson and D. Raulet, "Rae1 and H60 ligands of the NKG2D receptor stimulate tumour immunity.," *Nature*, vol. 413, pp. 165-71, 2001.
- [35] S. Halle, A. S. Keyser, F. R. Stahl and e. al., "In Vivo Killing Capacity of Cytotoxic T Cells Is Limited and Involves Dynamic Interactions and T Cell Cooperativity," *Immunity*, vol. 44, no. 2, pp. 233-245, 2016.
- [36] L. Gattinoni, S. Finkelstein, C. Klebanoff, P. Antony, D. Palmer and P. Spess, "Removal of

- homeostatic cytokine sinks by lymphodepletion enhances the efficacy of adoptively transferred tumor-specific CD8(+) T cells.," *Journal of Experimental Medicine* , vol. 202, 2005.
- [37] S. Sakaguchi, K. Wing, Y. Onishi, P. Prieto-Martin and T. Yamaguchi, "Regulatory T cells: how do they suppress immune responses?," *International Immunology*, vol. 21, pp. 1105-1111, 9 2009.
- [38] W. Cui and S. Kaech, " Generation of effector CD8+T cells and their conversion to memory T cells.," *Immunological Reviews* , vol. 236, pp. 151-66, 2010.
- [39] D. A. A. Vignali and L. W. W. C. J. Collison, "How regulatory T cells work," *Nat Rev Immunol*, vol. 8, no. 7, pp. 523-532, 2008.
- [40] I. Bains, R. Antia, R. Callard and A. Yates, "Quantifying the development of the peripheral naive CD4(+) T-cell pool in humans.," *Blood*, vol. 113, pp. 5480-7, 2009.
- [41] L. E. Richert-Spuhler and J. M. Lund, "The Immune Fulcrum: Regulatory T Cells Tip the Balance Between Pro- and Anti-inflammatory Outcomes upon Infection," *Prog Mol Biol Transl Sci*, vol. 136, pp. 217-243, 2015.
- [42] P. Antony, C. Piccirillo, A. Akpınarli, S. Finkelstein, P. Speiss, D. Surman, D. Palmer, C. Chan, C. Klebanoff, W. Overwijk, S. Rosenberg and N. Restifo, "CD8+ T cell immunity against a tumor/self-antigen is augmented by CD4+ T helper cells and hindered by naturally occurring T regulatory cells.," *J Immunol*, vol. 5, no. 174, pp. 2591-601, 2005.
- [43] G. Lythe, R. E. Callard, R. L. Hoare and C. Molina-Paris, "How many TCR clonotypes does a body maintain?," *J Theor Biol*, no. 389, pp. 214-224, 2016.
- [44] D. W. Kufe and P. P. Major, "5-fluorouracil incorporation into human breast carcinoma RNA correlates with cytotoxicity," *J. Biol. Chem.*, vol. 256, no. 19, pp. 9802-9805, 1981.
- [45] G. Arancia, A. Calcabrini, S. Meschini and A. Molinari, "Intracellular distribution of anthracyclines in drug resistant cells," *Cytotechnology*, vol. 27, pp. 95-111, 1998.
- [46] J. Hao, M. Madigan, A. Khatri, C. Power, T. Hung, J. Beretov, L. Chang, W. Xiao, P. Cozzi, P. Graham, J. Kearsley and Y. Li, "In Vitro and In Vivo Prostate Cancer Metastasis and Chemoresistance Can Be Modulated by Expression of either CD44 or CD147," *PLoS One*, vol. 7, no. 8, p. e40716, 2012.
- [47] R. Jain, J. Lee, C. Ng, D. Hong, J. Gong, A. Naing and e. al., "Change in Tumor Size by RECIST Correlates Linearly With Overall Survival in Phase I Oncology Studies.," *Journal of Clinical Oncology* , vol. 30, pp. 2684-90, 2012.
- [48] T. Arstila, A. Casrouge, V. Baron, J. Even, J. Kanellopoulos and P. Kourilsky, "A direct estimate of the human alphabeta T cell receptor diversity," *Science*, vol. 286, no. 5441, pp. 958-61, 1999.
- [49] M. Robertson-Tessi, R. Gillies, R. Gatenby and A. Anderson, "Impact of Metabolic Heterogeneity on Tumor Growth, Invasion, and Treatment Outcomes.," *Cancer Research* , vol. 75, pp. 1567-79, 2015.
- [50] G. Plosker, "Sipuleucel-T In Metastatic Castration-Resistant Prostate Cancer," *Drugs*, vol. 71, no. 1, pp. 101-8, 2011.
- [51] N. Sheikh, J. Cham, L. Zhang, T. DeVries, S. Letarte, J. Pufnock and e. al., " Clonotypic Diversification of Intratumoral T Cells Following Sipuleucel-T Treatment in Prostate Cancer Subjects," *Cancer Research*, vol. 76, pp. 3711-8, 2016.
- [52] M. Merad and M. Manz, " Dendritic cell homeostasis.," *Blood* , vol. 113, pp. 3418-27, 2009.
- [53] J. Crawford, D. Dale and G. Lyman, " Chemotherapy-induced neutropenia - Risks, consequences, and new directions for its management.," *Cancer*, vol. 100, pp. 228-37, 2004.
- [54] H. Wang, M. Li, J. Rinehart and R. Zhang, "Dexamethasone as a chemoprotectant in cancer chemotherapy: hematoprotective effects and altered pharmacokinetics and tissue distribution of carboplatin and gemcitabine.," *Cancer Chemotherapy and Pharmacology*, vol.

53, no. 6, pp. 459-67, 2004.

- [55] B. C. E, S. Tischer, J. Lahrberg, M. Oelke, C. Figueiredo, R. Blasczyk and B. Eiz-Vesper, "Granulocyte colony-stimulating factor impairs CD8+ T cell functionality by interfering with central activation elements," *Clin. Exp Immunol*, vol. 185, no. 1, pp. 107-118, 2016.
- [56] G. Freyer, N. Jovenin, G. Yazbek, C. Villanueva, A. Hussain, A. Berthune and e. al., "Granocyte-colony Stimulating Factor (G-CSF) Has Significant Efficacy as Secondary Prophylaxis of Chemotherapy-induced Neutropenia in Patients with Solid Tumors," *Anticancer Res*, vol. 33, no. 1, pp. 301-7, 2013.
- [57] E. S. Lugada, J. Mermin, F. Kaharuza, E. Ulvestad, W. Were, N. Lageland, B. Asjo, S. Malamba and R. Downing, "Population-Based Hematologic and Immunologic Reference Values for a Healthy Ugandan Population," *Clin. Diagn. Lab. Immunol.*, vol. 11, no. 1, pp. 29-34, 2004.
- [58] R. Kim, M. Emi and K. Tanabe, "Cancer immunoediting from immune surveillance to immune escape," *Immunology*, vol. 121, pp. 1-14, 2007.
- [59] A. Makkouk and G. Weiner, " Cancer Immunotherapy and Breaking Immune Tolerance: New Approaches to an Old Challenge.," *Cancer Research*, vol. 75, pp. 5-10, 2015.
- [60] H. Guo and K. Tsung, "Tumor reductive therapies and antitumor immunity," *Oncotarget*, vol. 8, no. 33, p. 55736–55749, 2017.
- [61] H. M. Mehta, M. Malandra and C. S. J, "G-CSF and GM-CSF in Neutropenia," *J Immunol*, vol. 195, no. 4, pp. 1341 - 1349, 2015.
- [62] S. Park, Z. Jiang, E. D. Mortenson, L. Deng, O. Radkevich-Brown, X. Yang, H. Sattar, Y. Wang, N. K. Brown, M. Greene, Y. Liu, J. Tang, S. Wang and Y.-X. Fu, "The Therapeutic Effect of Anti-HER2/neu Antibody Depends on Both Innate and Adaptive Immunity," *Cancer Cell*, vol. 18, no. 2, pp. 160-170, 2010.
- [63] R. L. Ferris, E. M. Jaffee and S. Ferrone, "Tumor Antigen–Targeted, Monoclonal Antibody–Based Immunotherapy: Clinical Response, Cellular Immunity, and Immunoescape," *J. Clin. Oncol.*, vol. 28, no. 28, pp. 4390-4399, 2010.
- [64] Y. Lee, S. L. Auh, Y. Wang, B. Burnette, Y. Wang, Y. Meng, M. Beckett, R. Sharma, R. Chin, T. Tu, R. R. Weichselbaum and Y.-X. Fu, "Therapeutic effects of ablative radiation on local tumor require CD8+ T cells: changing strategies for cancer treatment," *Blood*, vol. 114, pp. 589-595, 2009.

727  
 728  
 729  
 730  
 731  
 732  
 733  
 734  
 735  
 736  
 737  
 738  
 739  
 740  
 741

742

Parameter	Symbol	Value	Literature reference
Tumor Growth Coefficient	$r_T$	1000 cells <sup>1-m</sup> day <sup>-1</sup>	[29]
CTL kill rate	$k_0$	1 day <sup>-1</sup>	[34], [35]
Treg suppression efficacy	$b$	0.75	[29]
Tumor growth transition size	$T_{trans}$	10 <sup>6</sup> cells	[49]
Power-Law growth exponent	$m$	0.5	[29]
Exponential to power smoothing term	$P$	3.0	[29]
Time till immune contraction	$t_{off}$	4-8 days	[16] [8] [14]
Maximum sustainable number of effector, naïve, and memory cells	$E_{max}$	10 <sup>12</sup> cells	[40]
Tumor antigenicity	$\alpha$	1*	[29]
CTL death/ apoptosis rate	$\delta_E$	0.05*	[39]
CTL contraction rate	$\rho$	0.13	[16]
CTL contraction augmentation due to Tregs	$c$	0.01*	[29]
Memory cell expansion factor	$\gamma$	100*	[16, 48]
Tumor-mediated Treg recruitment rate	$\sigma$	0.01	[42, 29]
Treg death rate	$\delta_R$	0.1*	[29]
Memory cell growth rate	$r_M$	0.01 day <sup>-1</sup> *	[40]
Memory cell reversion rate	$\omega$	0.01*	[40]
Naïve cell growth rate	$r_N$	0.1 day <sup>-1</sup>	[40]
Maximum number of naïve T cells and memory cells	$K_{max}$	10 <sup>12</sup> cells	[43]
Baseline chemotherapy strength	$C_0$	Varied in simulation	

743

744

745

746

747

748

749

750

**Table 1:** Model parameters were estimated based upon both pre-existing models, chiefly Althaus *et al.*, 2007 and Robertson-Tessi *et al.*, 2012, as well as experimental studies. For some parameters, the literature often indicated significant variation, so order-of-magnitude approximations were made. Similarly, certain parameters were not succinctly captured in literature studies and were therefore estimated (\*). We have addressed the impact of potential parameter variation through sensitivity studies (see Results).

## Figure Legends

**Figure 1:** Tumor-immune dynamics during the sensitive (A) and tolerant (B) stages of the immune response. During antigen-sensitive immune expansion, CTLs are recruited from memory cells to attack tumor cells. Tregs are being recruited but have not yet started significantly inhibiting CTL responses. During immune contraction once tolerance sets in, Tregs exert an active inhibitory pressure on CTLs. Expansion of memory cells into CTLs ceases. Both stages of the immune response are characterized by competition between memory and naïve immune cells for common cytokine pools as well as homeostatic proliferation and lymphopoiesis.

**Figure 2:** Interaction of memory-cell populations and chemotherapy strength on treatment outcomes. RECIST outcomes are shown in panel A with progressive disease (red), stable disease (yellow), partial response (light blue) and complete response (dark blue). (B) Finer grade responses are shown as percent changes in tumor size after therapy versus the initial starting size ( $10^8$  cells). The underlying dynamic reasons for these differences can be seen in the memory populations during low (C) and high dose chemotherapy (D). Low dose chemotherapy allows memory populations (light blue) to be sustained for longer and generate larger CTL responses (green). High dose chemotherapy, however, depletes memory cells faster and leads to declining CTL responses and concurrent tumor escape.

**Figure 3:** Treatment outcomes for variation in tumor growth rate (A and B) and CTL efficacy (C and D). Panels A and C represent RECIST outcomes. Red is progressive disease (PD), dark blue is complete response (CR), light blue is partial response (PR) and yellow is stable disease (SD). Treatment outcomes with faster growing tumors are more sensitive to maintaining chemotherapy dosing in the Goldilocks Window. For slower growing tumors, treatment outcomes are more successful and less sensitive to dose. Similarly, more efficient patient CTLs lead to more successful outcomes and have less dependence on chemotherapy. However, outcomes become more sensitive to dosing for patients with less efficiently killing CTLs.

**Figure 4:** Improvements in tumor reduction due to vaccine application. Panel A shows the RECIST responses achieved for different vaccine strengths and chemotherapy strengths with black being the non-vaccine baseline. Vaccine strengths ( $v$ ) are 1 (blue), 10 (green), 100 (red), 1000 (light blue). Larger vaccine strengths lead to more successful RECIST responses for stronger chemotherapy doses. When looking at the absolute number of improvement in cellular reduction (B), a window of optimal chemotherapy ranges appears. Only when chemotherapy is in this range can vaccines provide a significant additional benefit.

**Figure 5:** Therapeutic effects of differential response to immune prophylactics. (A) Final tumor sizes are shown for three different chemotherapy regimes ( $C = 0.25$  as blue,  $C = 0.6$  as green, and  $C = 0.9$  as red) for a range of immune modifier efficacies ( $h$ ). The asterisk denotes that simulations were only run up to this  $h$  value for the highest dose chemotherapy. The dotted line represents the tumor size at the start of therapy. (B) Cohorts are treated with these differing regimes of high and low chemotherapy, showing significant differences in the proportion of successful versus unsuccessful responders.

**Figure 6:** A diagram explaining tumor outcomes at varying chemotherapy strengths and immune support doses. If therapy is too weak, then immune stimulation cannot be maximally effective and direct chemotherapy-mediated tumor cell death is also low. This yields a suboptimal tumor reduction. When chemotherapy is too strong, there may be more tumor cell death due to the drug, but insufficient immune activation due to over depletion of T cells. There is a moderate dose, however, that represents a Goldilocks Window of maximizing both T-cell activation as well as drug-

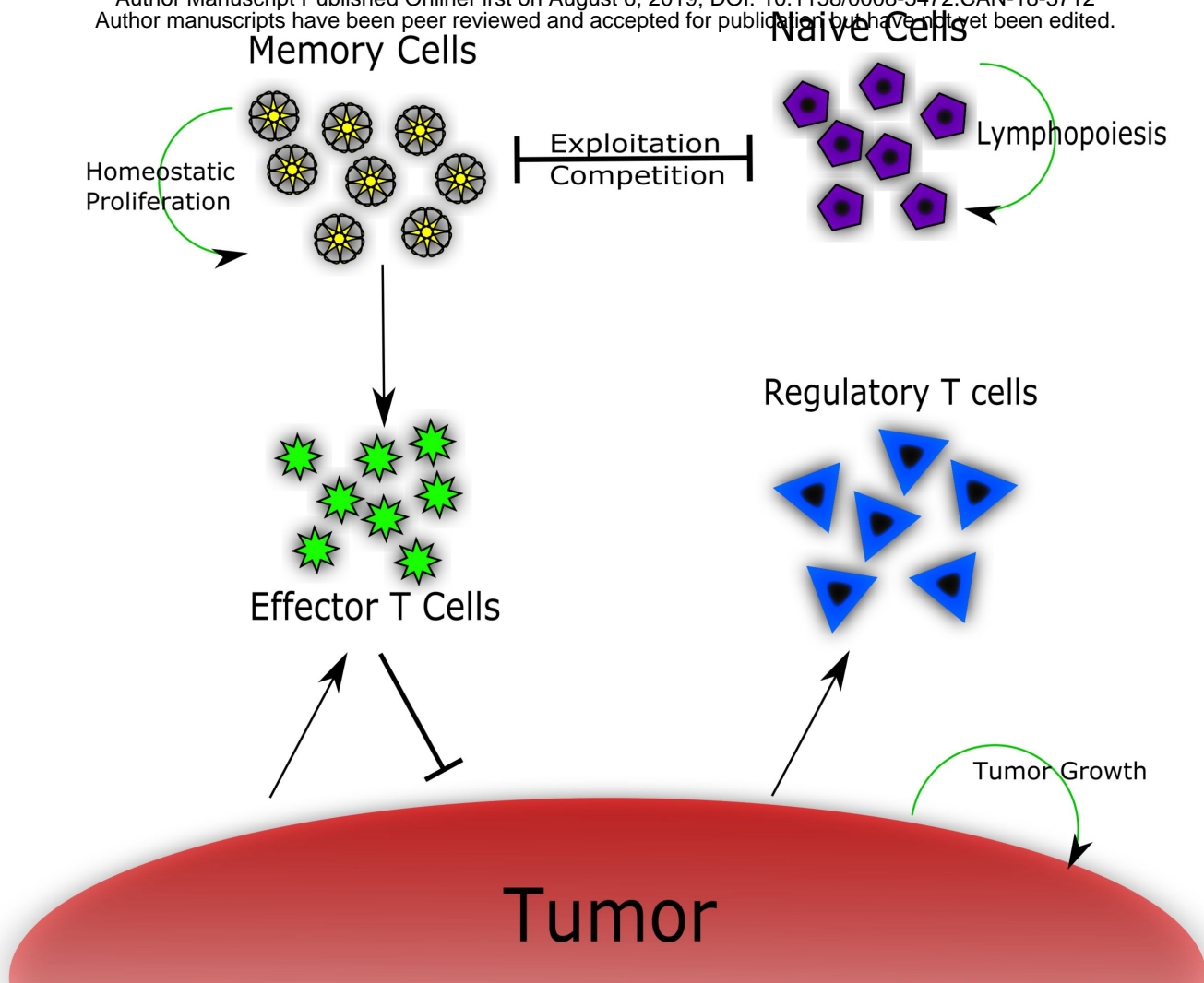
803 induced tumor cell death. This range of dosing provides at least a 20% reduction in tumor size  
804 (relative to the initial tumor size of  $10^8$  cells).  
805  
806



# Figure 1

A

Author Manuscript Published OnlineFirst on August 6, 2019; DOI: 10.1158/0008-5472.CAN-18-3712  
Author manuscripts have been peer reviewed and accepted for publication, but have not yet been edited.



B

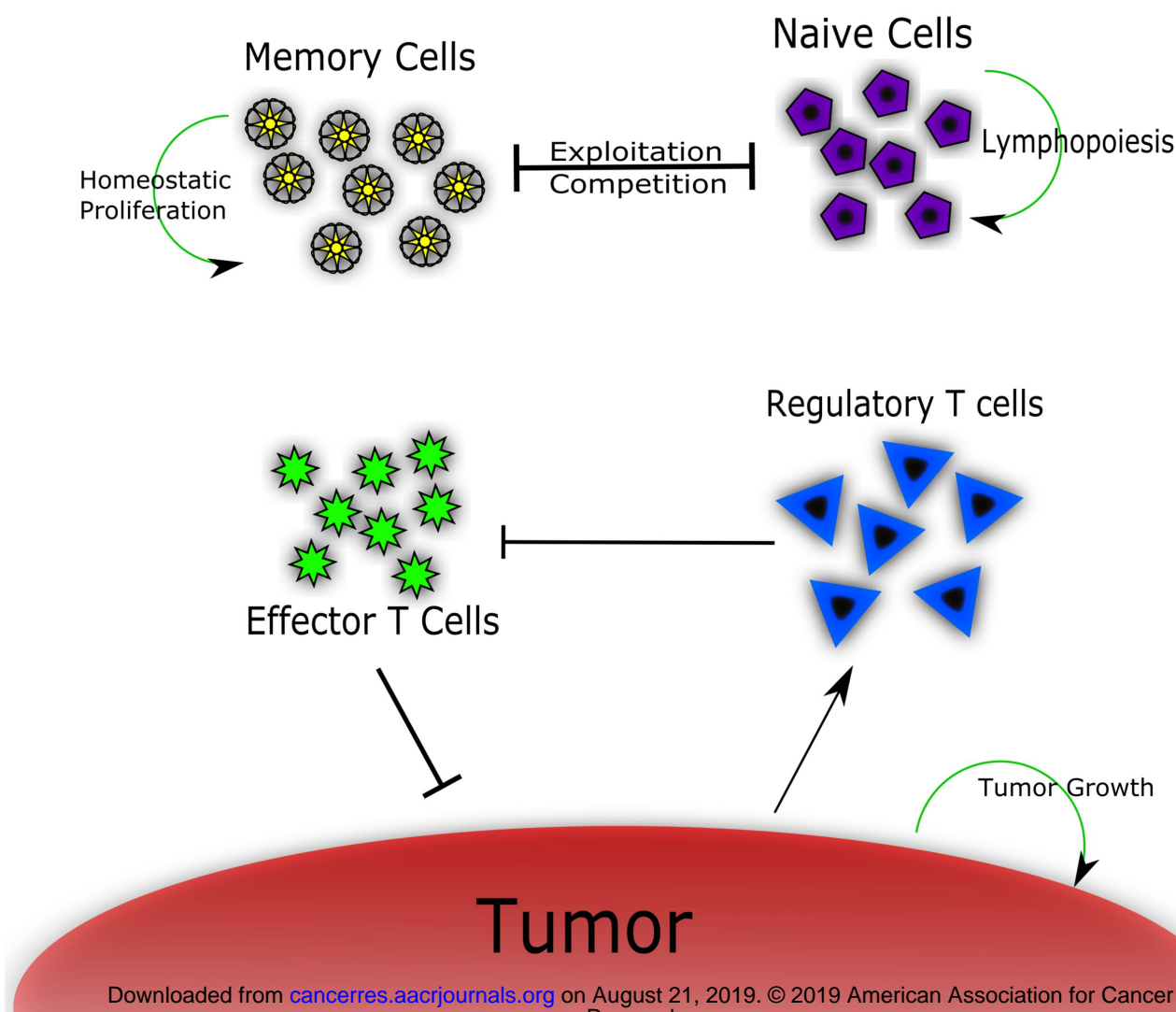


Figure 2

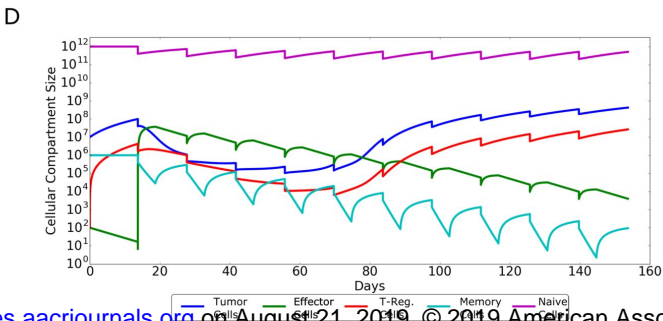
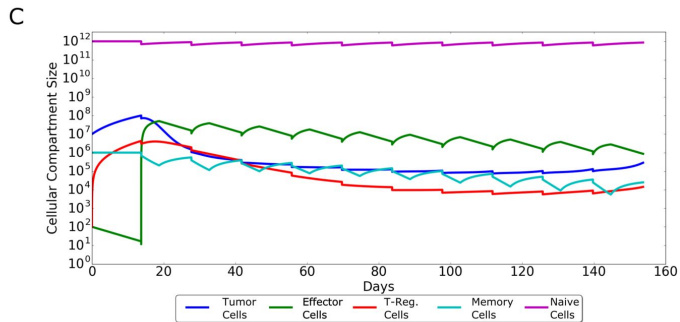
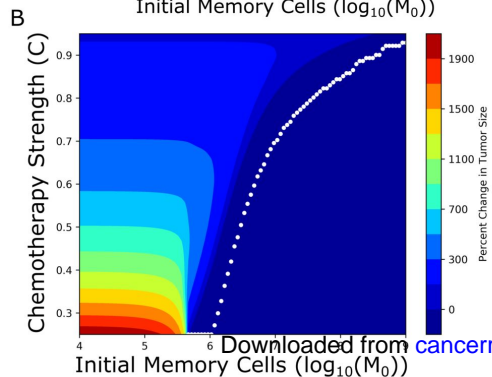
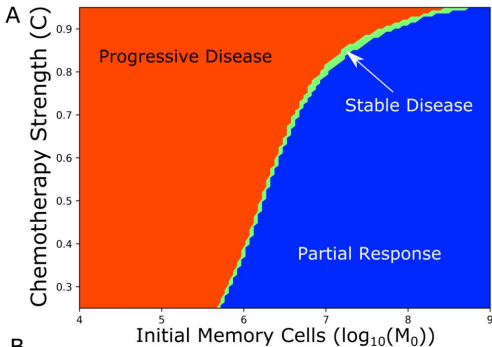




Figure 3

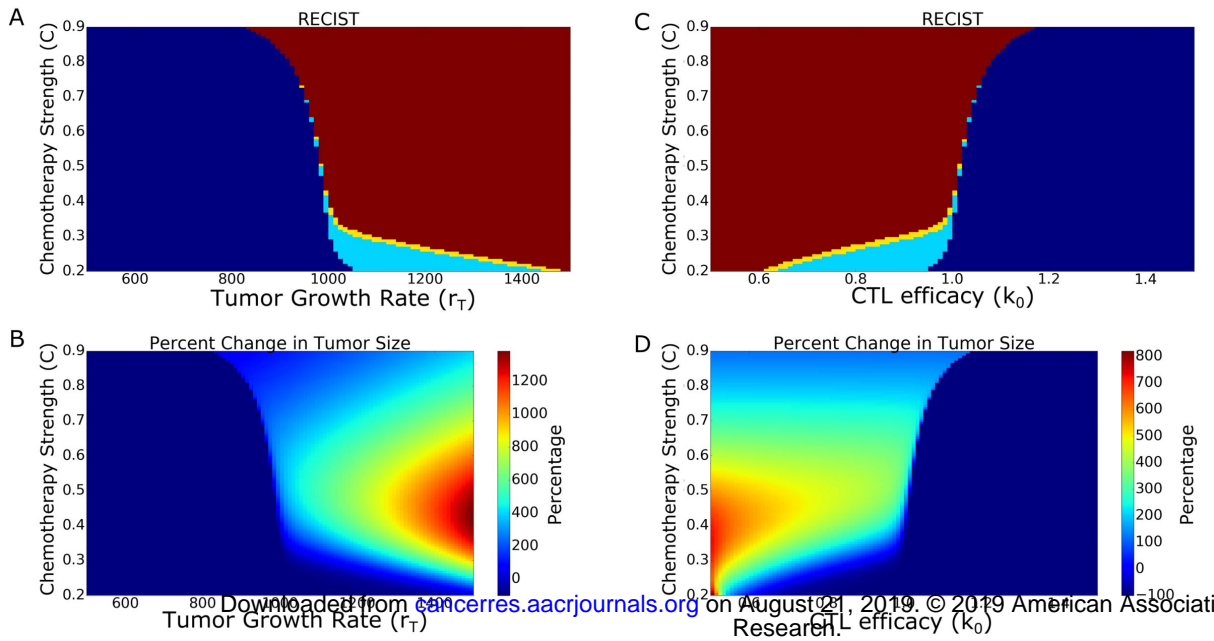
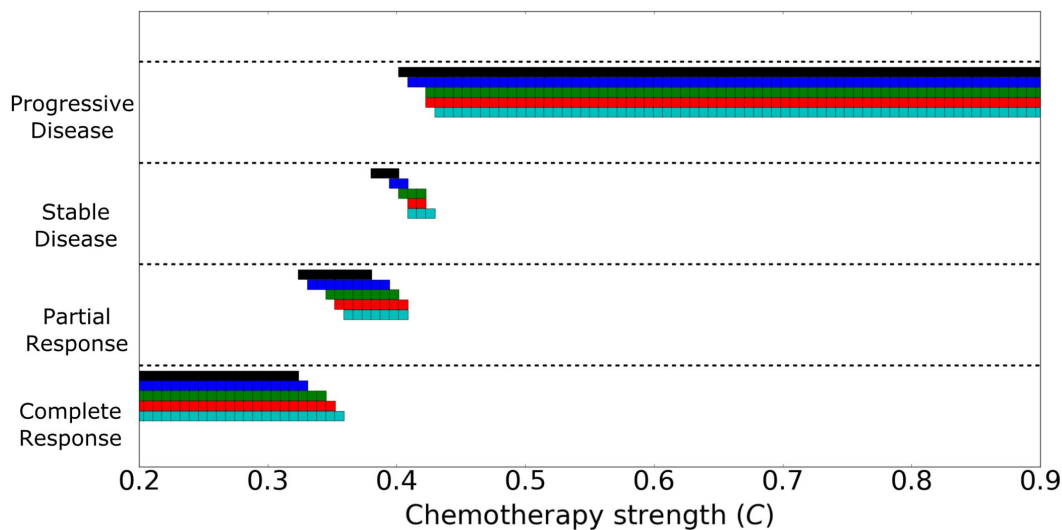


Figure 4

A



B

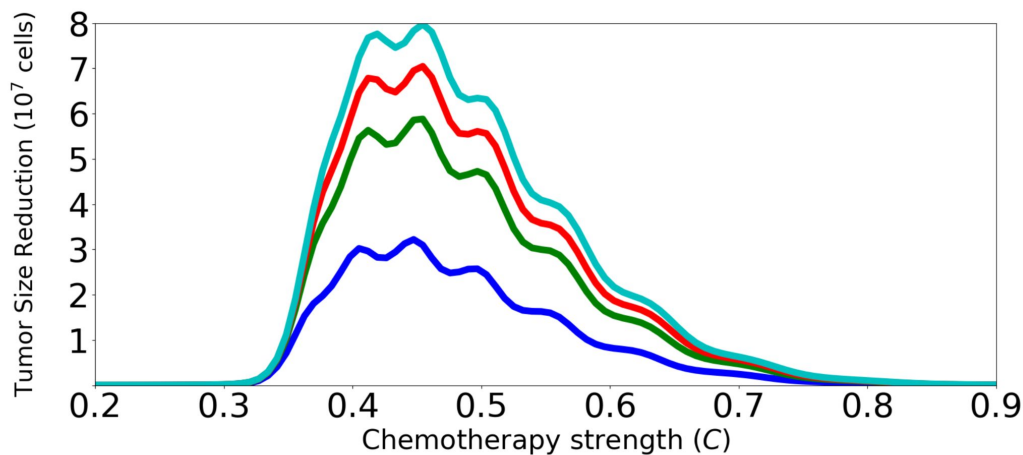
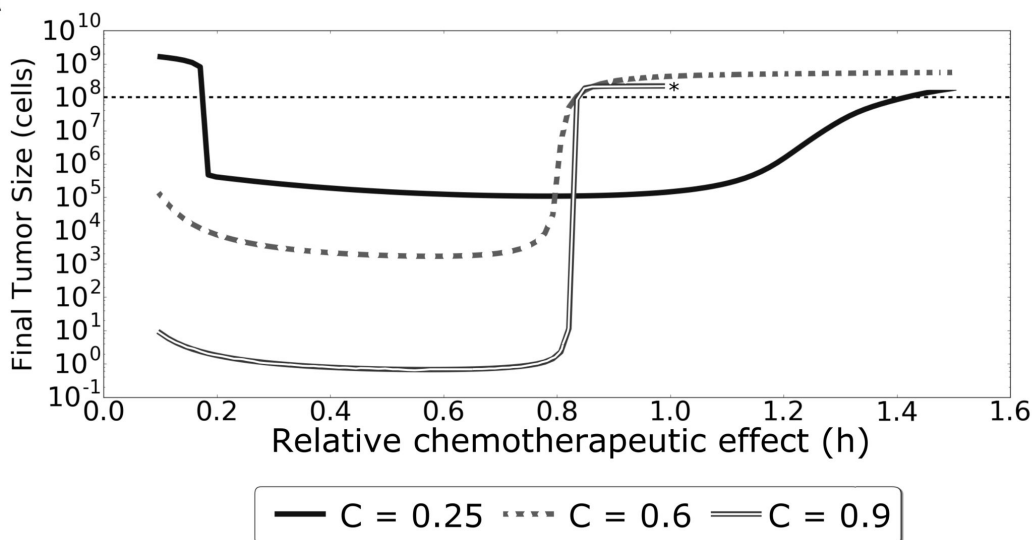


Figure 5

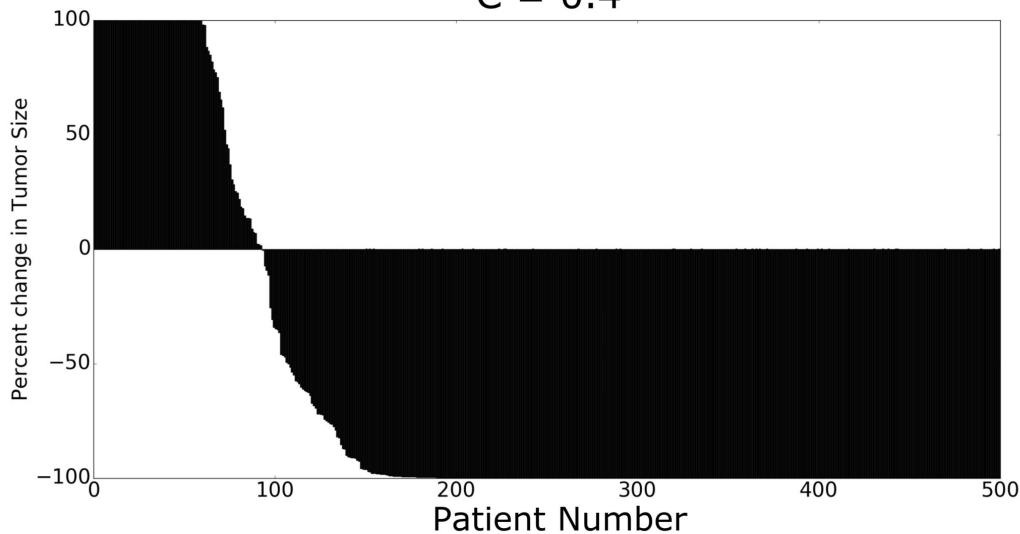
A



## Cohort Responses to Chemotherapy

B

C = 0.4



C = 0.9

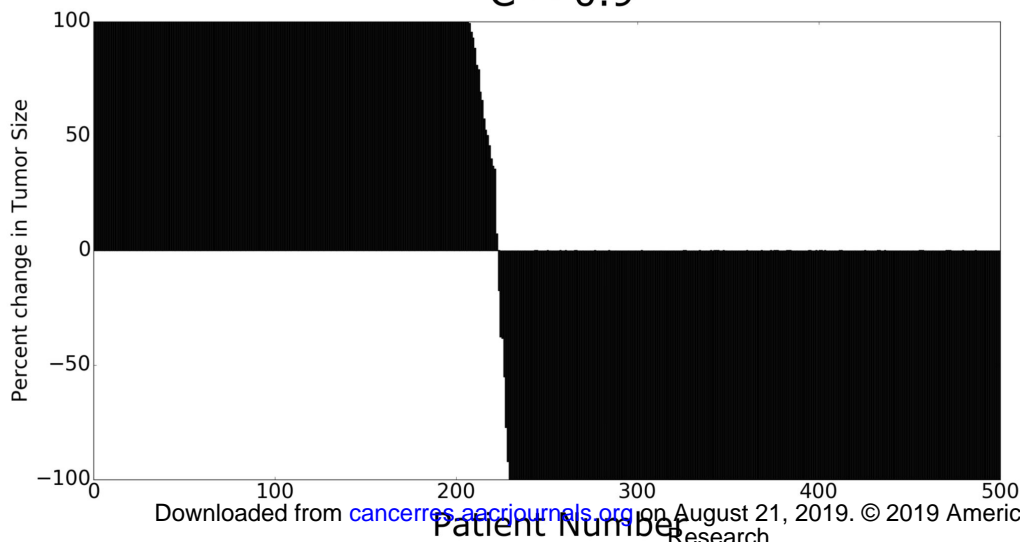


Figure 6

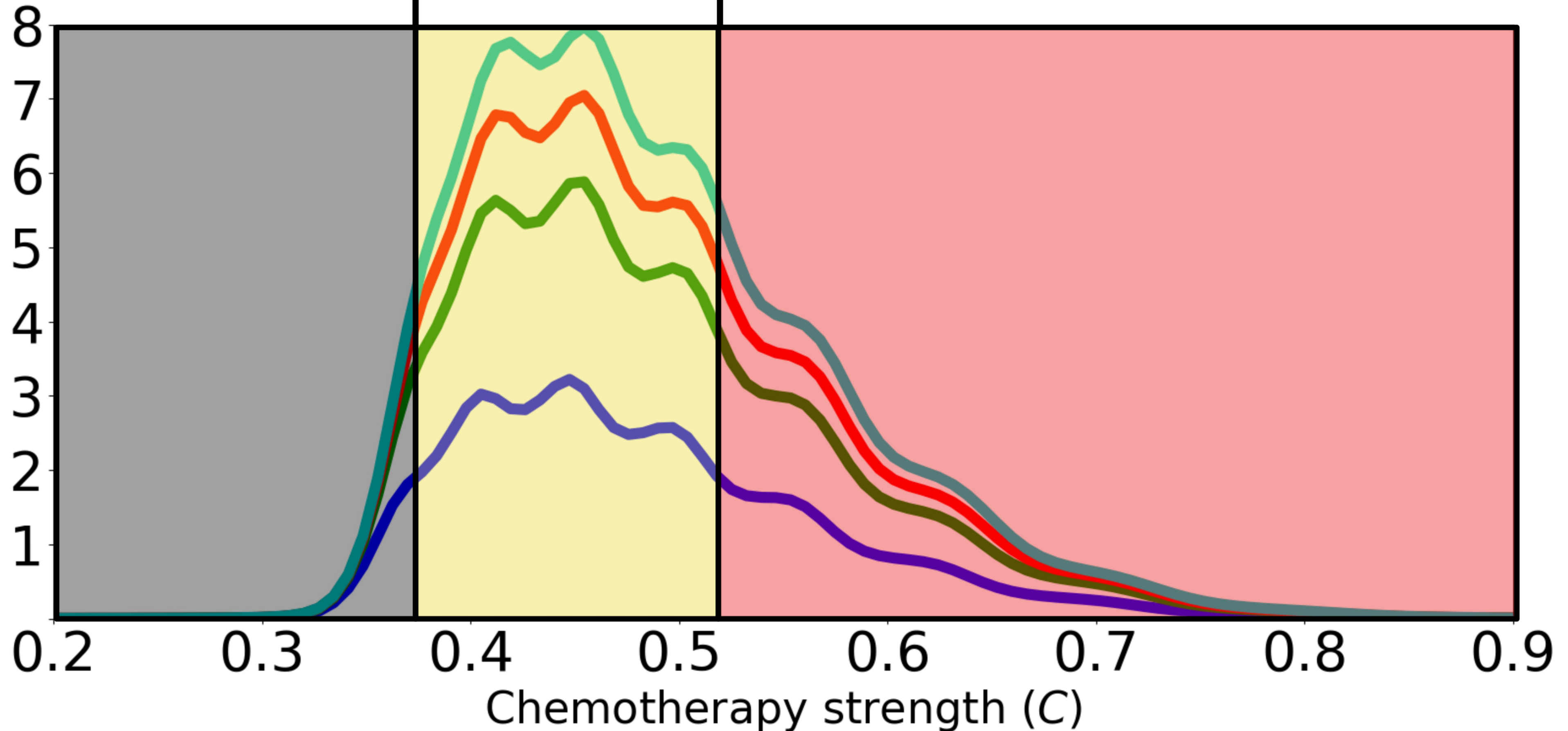
Insufficient  
Chemotherapy

Goldilocks  
Window

Overly Immunodepleting  
Chemotherapy

Author Manuscript Published OnlineFirst on August 6, 2019; DOI: 10.1158/0008-5472.CAN-18-3712  
Author manuscripts have been peer reviewed and accepted for publication but have not yet been edited.

Tumor Size Reduction ( $10^7$  cells)



$v = 1$        $v = 10$        $v = 100$        $v = 1000$

# Cancer Research

The Journal of Cancer Research (1916–1930) | The American Journal of Cancer (1931–1940)

## The Goldilocks Window of Personalized Chemotherapy: Getting the Immune Response Just Right

Derek S Park, Mark Robertson-Tessi, Kimberly A Luddy, et al.

*Cancer Res* Published OnlineFirst August 6, 2019.

<b>Updated version</b>	Access the most recent version of this article at: doi: <a href="https://doi.org/10.1158/0008-5472.CAN-18-3712">10.1158/0008-5472.CAN-18-3712</a>
<b>Supplementary Material</b>	Access the most recent supplemental material at: <a href="http://cancerres.aacrjournals.org/content/suppl/2019/08/06/0008-5472.CAN-18-3712.DC1">http://cancerres.aacrjournals.org/content/suppl/2019/08/06/0008-5472.CAN-18-3712.DC1</a>
<b>Author Manuscript</b>	Author manuscripts have been peer reviewed and accepted for publication but have not yet been edited.

<b>E-mail alerts</b>	<a href="#">Sign up to receive free email-alerts</a> related to this article or journal.
<b>Reprints and Subscriptions</b>	To order reprints of this article or to subscribe to the journal, contact the AACR Publications Department at <a href="mailto:pubs@aacr.org">pubs@aacr.org</a> .
<b>Permissions</b>	To request permission to re-use all or part of this article, use this link <a href="http://cancerres.aacrjournals.org/content/early/2019/08/06/0008-5472.CAN-18-3712">http://cancerres.aacrjournals.org/content/early/2019/08/06/0008-5472.CAN-18-3712</a> . Click on "Request Permissions" which will take you to the Copyright Clearance Center's (CCC) Rightslink site.